On the Color Dipole Picture

Dieter Schildknecht

Universität Bielefeld & Max Planck Institut für Physik, München

Diffraction 2016

Acireale (Catania, Sicily), September 2 – 8, 2016

1. **Deep Inelastic ep Scattering**

2. **J/Ψ and Y Production**

3. **Ultrahigh-energy Neutrino Interaction**

4. **Conclusions**

1. Deep Inelastic ep Scattering

Experimental Results

Deep inelastic scattering (DIS), HERA 1992 to 2007:

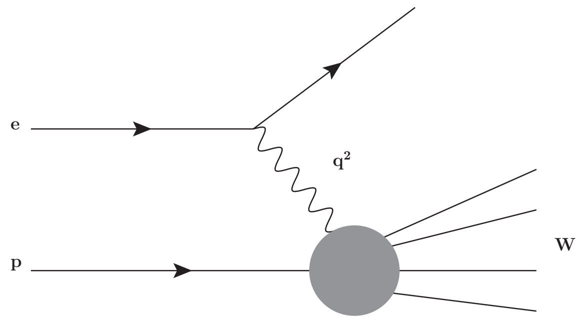

DIS at low values of

$$x \equiv x_{bj} \simeq \frac{Q^2}{W^2}, \text{ where}$$
$$5 \cdot 10^{-4} \leq x \leq 10^{-1}$$
$$0 \leq Q^2 \leq 100 GeV^2$$

$$\begin{aligned} Q^2 &\equiv -q^2 > 0, \\ x_{bj} &= \frac{Q^2}{W^2 + Q^2 + M_p^2} \cong \frac{Q^2}{W^2}. \end{aligned}$$

$$\begin{aligned} \sigma_{\gamma^* p}(W^2, Q^2) &= \sigma_{\gamma_L^* p}(W^2, Q^2) + \sigma_{\gamma_T^* p}(W^2, Q^2) \\ &\equiv \sigma_{\gamma_T^* p}(W^2, Q^2)(1 + R(W^2, Q^2)), \end{aligned}$$

$$\begin{aligned} F_2(x, Q^2) &\cong \frac{Q^2}{4\pi^2 \alpha} \sigma_{\gamma^* p}(W \cong \frac{Q^2}{x}, Q^2); \\ F_L &= \frac{R}{1+R} F_2. \end{aligned}$$

Low-x Scaling

Empirically : $\eta(W^2, Q^2) \equiv \dfrac{Q^2 + m_0^2}{\Lambda_{sat}^2(W^2)},$

$\Lambda_{sat}^2(W^2) \sim (W^2)^{C_2}$

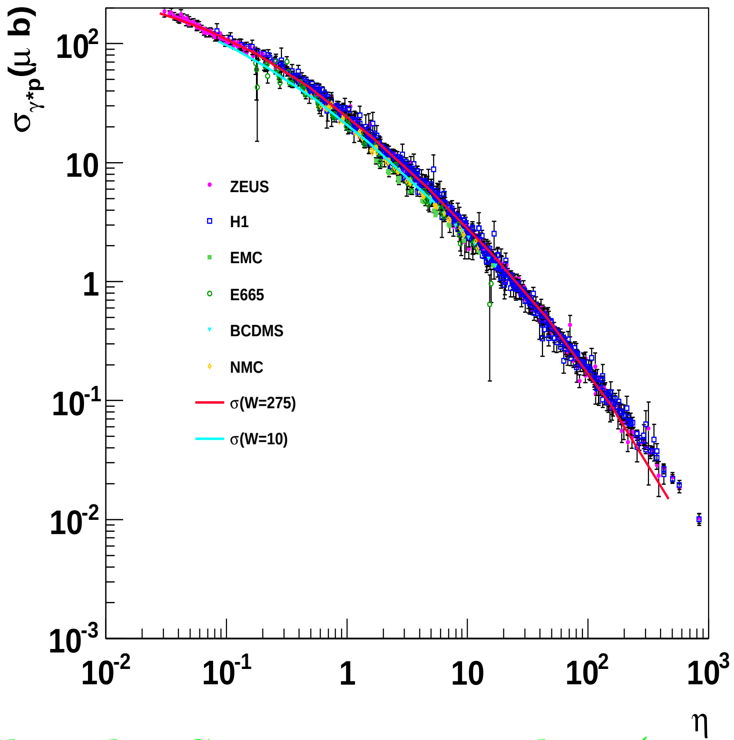

Schildknecht, Surrow, Tentyukov (2000)

$$\sigma_{\gamma^* p}(W^2, Q^2) \;=\; \sigma_{\gamma^* p}(\eta(W^2, Q^2))$$

$$\sim\; \sigma^{(\infty)} \begin{cases} ln\frac{1}{\eta(W^2,Q^2)} & , \quad \text{for } \eta(W^2, Q^2) \ll 1 \\ \frac{1}{\eta(W^2,Q^2)} & , \quad \text{for } \eta(W^2, Q^2) \gg 1 \end{cases}$$

The W-dependence

$$F_2(x, Q^2) \cong \frac{Q^2}{4\pi^2\alpha}\left(\sigma_{\gamma^*_L p}(W^2, Q^2) + \sigma_{\gamma^*_T p}(W^2, Q^2)\right)$$

$$= F_2(W^2) \text{ for } x < 0.1. \qquad (10GeV^2 \leq Q^2 \leq 100GeV^2)$$

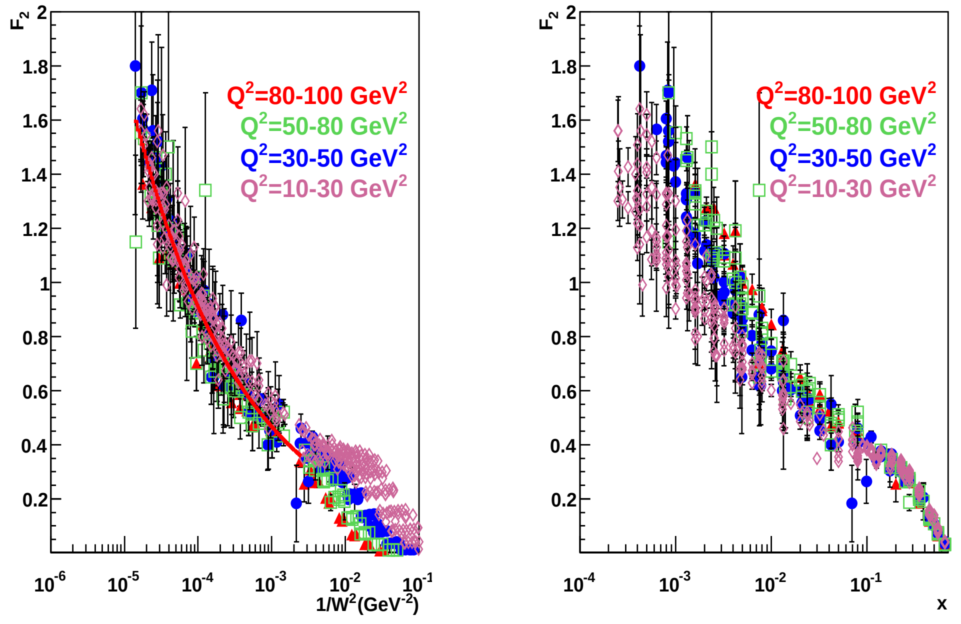

$$F_2(W^2) = f_2\left(\frac{W^2}{1GeV^2}\right)^{c_2=0.29},$$

$$f_2 = 0.063.$$

Kuroda, Schildknecht (2010)

(Prabhdeep Kaur)

The limit of $\eta(W^2,Q^2) \to 0$, or $W^2 \to \infty$ at Q^2 fixed ("saturation")

$$\lim_{\substack{W^2\to\infty \\ Q^2 \text{ fixed}}} \frac{\sigma_{\gamma^* p}(\eta(W^2,Q^2))}{\sigma_{\gamma^* p}(\eta(W^2,Q^2=0))} = \lim_{\substack{W^2\to\infty \\ Q^2 \text{ fixed}}} \frac{\ln\left(\frac{\Lambda^2_{sat}(W^2)}{m_0^2}\frac{m_0^2}{(Q^2+m_0^2)}\right)}{\ln\frac{\Lambda^2_{sat}(W^2)}{m_0^2}} = 1 + \lim_{\substack{W^2\to\infty \\ Q^2 \text{ fixed}}} \frac{\ln\frac{m_0^2}{Q^2+m_0^2}}{\ln\frac{\Lambda^2_{sat}(W^2)}{m_0^2}} = 1.$$

$$\sigma_{\gamma^* p}\left(\eta(W^2,Q^2=0)\right) = \sigma_{\gamma p}(W^2)$$

D. Schildknecht, DIS 2001 (Bologna)

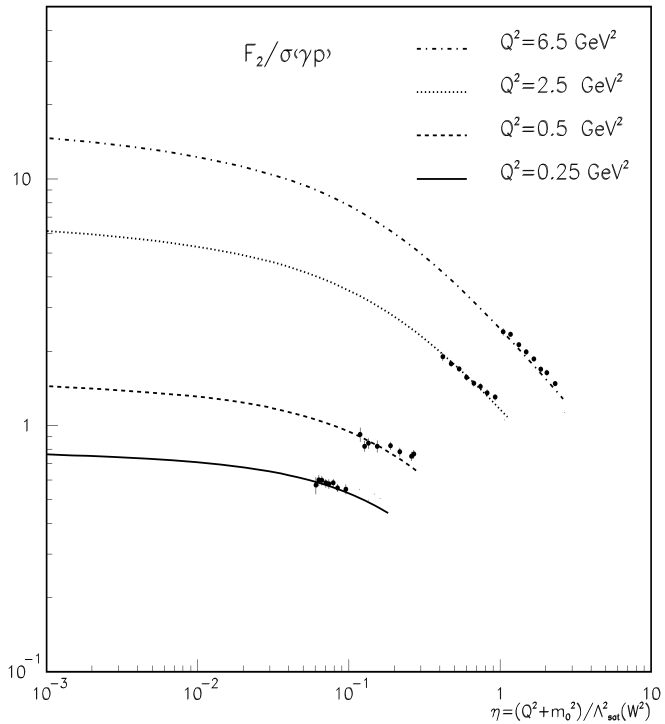

$$\lim_{\substack{W^2\to\infty \\ Q^2 \text{fixed}}} \frac{F_2(x\cong Q^2/W^2,Q^2)}{\sigma_{\gamma p}(W^2)} = \frac{Q^2}{4\pi^2\alpha}.$$

Q^2[GeV^2]	W^2[GeV^2]	$\frac{\sigma_{\gamma^* p}(\eta(W^2,Q^2))}{\sigma_{\gamma p}(W^2)}$
1.5	2.5×10^7	0.5
	1.26×10^{11}	0.63

for $\eta = 10^{-2}$:

Q^2[GeV^2]	$\Lambda^2_{sat}(W^2)$[GeV^2]	W[GeV]
0.5	65	1.7×10^4
2.5	265	2.2×10^5

VHEeP: W $\sim 10^4$GeV

The experimentally observed behavior

follows from the Color Dipole Picture (CDP)

of deep-inelastic scattering for $x \lesssim 0.1$.

The Color Dipole Picture (CDP).

The longitudinal and the transverse photoabsorption cross section

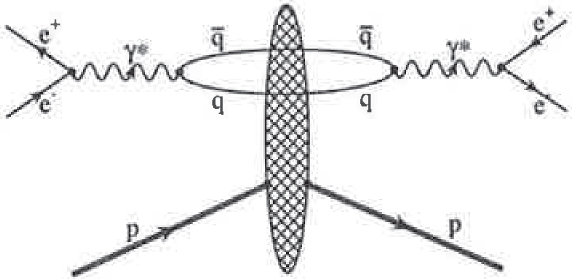

(a)

channel 1:

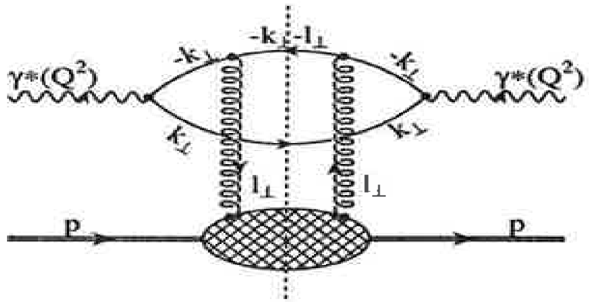

(a)

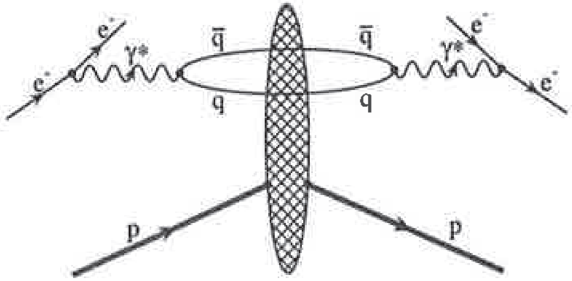

(b)

channel 2:

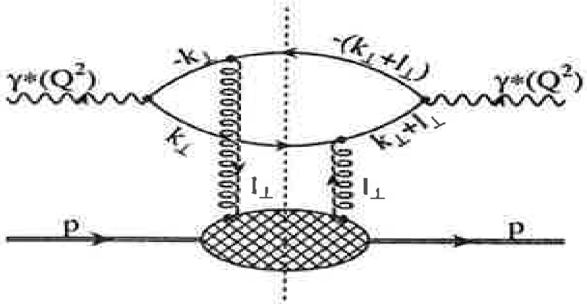

(b)

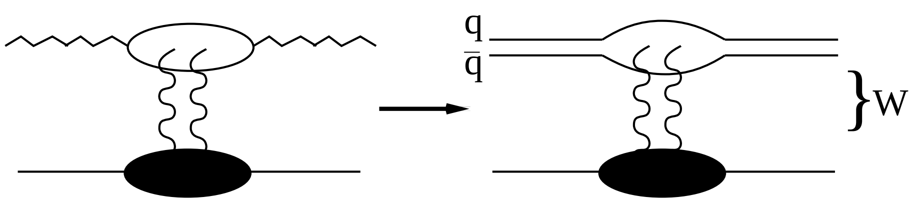

$\gamma^* p \to \gamma^* p \longrightarrow (q\bar{q})p \to (q\bar{q})p$

$$\tau = \frac{1}{\Delta E} \cong \frac{1}{x + \frac{M^2_{q\bar{q}}}{W^2}} \frac{1}{M_p} \gg \frac{1}{M_p}$$

A) $\boldsymbol{\sigma_{\gamma^*_{L,T}}(W^2, Q^2) = \int dz \int d^2\vec{r}_\perp |\psi_{L,T}(\vec{r}_\perp, z(1-z), Q^2)|^2 \;\; \sigma_{(q\bar{q})p}(\vec{r}_\perp, z(1-z), W^2)}$

Remarks:

i) $|\psi_{L,T}(\vec{r}_\perp, z(1-z), Q^2)|$: **Probability for** $\gamma^*_{L,T} \to q\bar{q}$ **fluctuation (QED)**

Note: $\vec{r}_\perp{}^2 \sim \frac{1}{Q^2}$

ii) $\sigma_{(q\bar{q})p}(\vec{r}_\perp, z(1-z), W^2)$: $(q\bar{q})p$ **cross section dependent on** W^2 **(not on** $x \equiv \frac{Q^2}{W^2}$**)**

Generalized Vector Dominance

Sakurai, Schildknecht 1972

B) Gauge-invariant two-gluon coupling (QCD):

$$\sigma_{(q\bar{q})p}(\vec{r}_\perp, z(1-z), W^2) = \int d^2\vec{l}_\perp \tilde{\sigma}(\vec{l}_\perp^{\,2}, z(1-z), W^2)\left(1 - e^{-i\,\vec{l}_\perp\cdot\vec{r}_\perp}\right)$$

Low (1975)
Nussinov (1975)
Nikolaev, Zakharov (1991)
Cvetic, Schildknecht, Shoshi(2000)

Assume $\vec{l}_\perp^{2} \leq \vec{l}_{\perp\mathrm{Max}}^{2}(W^2)$.

For fixed $|\vec{r}_\perp|$:

a) $\vec{l}_{\perp\mathrm{Max}}^{2}(W^2)\vec{r}_\perp^{2} \ll 1$

$\sigma_{(q\bar{q})p} \sim \vec{r}_\perp^{2}$, "color transparency", $\xrightarrow[(A)]{} \sigma_{\gamma^* p} \sim \frac{1}{\eta(W^2,Q^2)} \sim \frac{\Lambda^2_{\mathrm{sat}}(W^2)}{Q^2}$.

b) $\vec{l}_{\perp\mathrm{Max}}^{2}(W^2)\vec{r}_\perp^{2} \gg 1$

$\sigma_{(q\bar{q})p} \sim \sigma^{(\infty)}(W^2)$, "saturation" $\xrightarrow[(A)]{} \sigma_{\gamma^* p} \sim \ln \frac{1}{\eta(W^2,Q^2)}$;

Color gauge invariant $q\bar{q}$ (dipole) interaction with gluon field in the nucleon implies low-x scaling.

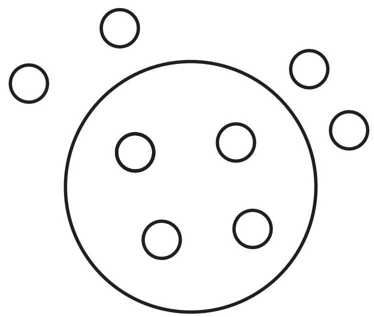

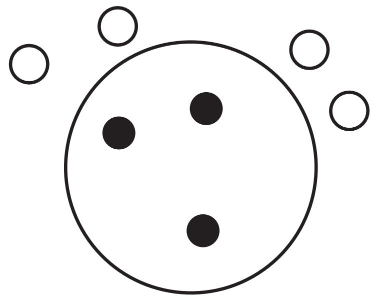

Color Transparency

$$\eta(W^2, Q^2) \simeq \frac{Q^2}{\Lambda^2_{\rm sat}(W^2)} \gg 1$$

Saturation

hadron-like cross section

$$\eta(W^2, Q^2) \lesssim 1$$

The (Q^2, W^2) plane of low-x DIS in CDP.

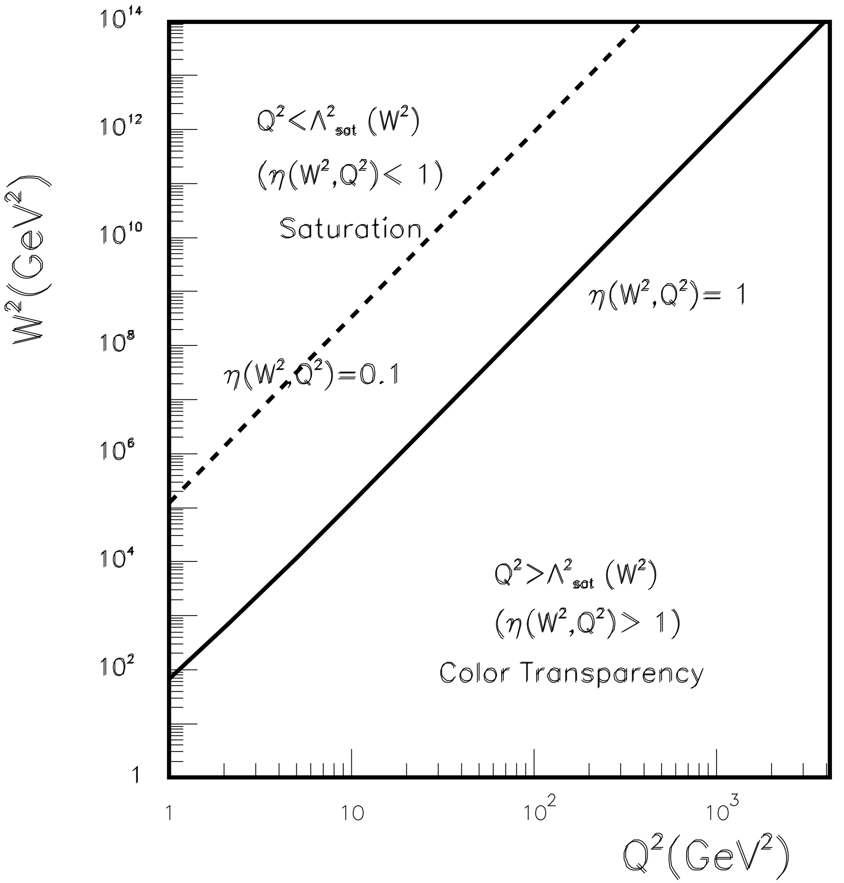

The longitudinal-to-transverse ratio

$(q\bar{q})^{J=1}_{L,T}$ states : $\gamma^*_{L,T} \to (q\bar{q})^{J=1}_{L,T}$

$$\sigma_{\gamma^*_{L,T}p}(W^2, Q^2) = \alpha \sum_q Q_q^2 \frac{1}{Q^2} \frac{1}{6} \begin{cases} \int d\vec{l}_\perp^{\prime 2} \vec{l}_\perp^{\prime 2} \bar{\sigma}_{(q\bar{q})^{J=1}_L p}(\vec{l}_\perp^{\prime 2}, W^2), \\ 2 \int d\vec{l}_\perp^{\prime 2} \vec{l}_\perp^{\prime 2} \bar{\sigma}_{(q\bar{q})^{J=1}_T p}(\vec{l}_\perp^{\prime 2}, W^2). \end{cases} \qquad (\text{for } \eta \gg 1)$$

$$\vec{l}^2 = z(1-z)\vec{l}_\perp^{\,2}$$

$$\rho_W = \frac{\int d\vec{l}_\perp^{\prime 2} \vec{l}_\perp^{\prime 2} \bar{\sigma}_{(q\bar{q})^{J=1}_T p}(\vec{l}_\perp^{\prime 2}, W^2)}{\int d\vec{l}_\perp^{\prime 2} \vec{l}_\perp^{\prime 2} \bar{\sigma}_{(q\bar{q})^{J=1}_L p}(\vec{l}_\perp^{\prime 2}, W^2)}. \equiv \rho$$

$$R = \frac{1}{2\rho}.$$

Magnitude of ρ

Average transverse momentum of $q(\bar{q})$:

$$\langle \vec{l}_\perp^{\,2} \rangle_{L,T}^{\vec{l}_\perp^{\,\prime 2}=const} = \vec{l}_\perp^{\,\prime 2} \begin{cases} 6 \int dz z^2 (1-z)^2 = \frac{4}{20} \vec{l}_\perp^{\,\prime 2}, & (L) \\ \frac{3}{2} \int dz \; z(1-z)(1-2z(1-z)) = \frac{3}{20} \vec{l}_\perp^{\,\prime 2}, & (T) \end{cases} .$$

Assume that ρ is determined by average transverse size of $L(T)$. Uncertainty principle:

$$\rho = \frac{\langle \vec{r}_\perp^{\,2} \rangle_T}{\langle \vec{r}_\perp^{\,2} \rangle_L} = \frac{\langle \vec{l}_\perp^{\,2} \rangle_L}{\langle \vec{l}_\perp^{\,2} \rangle_T} = \frac{4}{3}.$$

Kuroda, Schildknecht (2008)

$$R = \frac{1}{2\rho} = \begin{cases} 0.5 & \text{for } \rho = 1, \\ \frac{1\cdot 3}{2\cdot 4} = \frac{3}{8} = 0.375 & \text{uncertainty principle} \\ \frac{1}{4}, & \text{for } \rho = 2. \end{cases}$$

$$F_L = \frac{R}{1+R} = \begin{cases} 0.33 \\ 0.27 \\ 0.20 \end{cases}$$

$$F_L = 0.27 F_2.$$

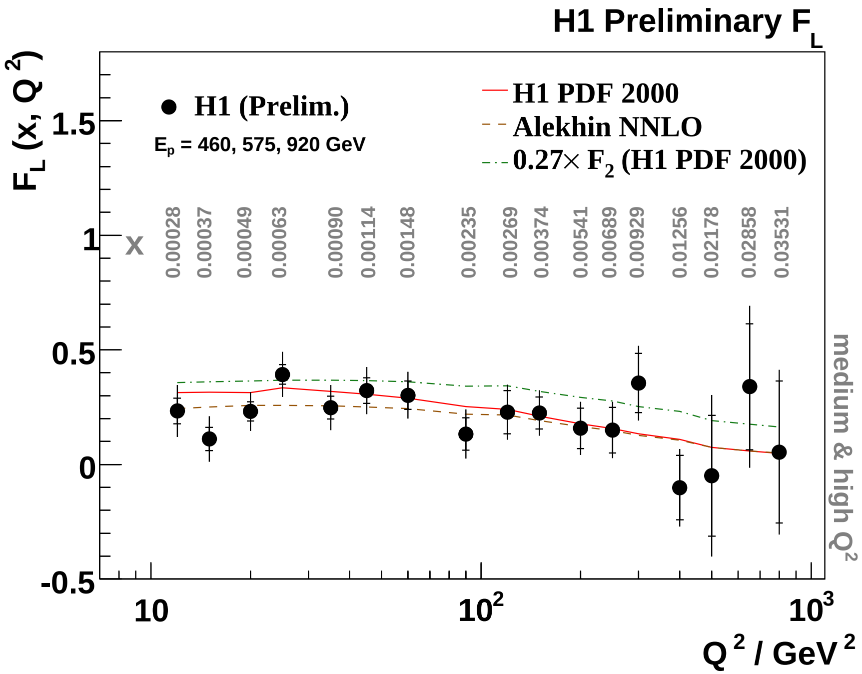
H1 Preliminary F_L
F_L (x, Q^2)
H1 (Prelim.)
E_p = 460, 575, 920 GeV
H1 PDF 2000
Alekhin NNLO
0.27× F_2 (H1 PDF 2000)
x
0.00028
0.00037
0.00049
0.00063
0.00090
0.00114
0.00148
0.00235
0.00269
0.00374
0.00541
0.00689
0.00929
0.01256
0.02178
0.02858
0.03531
medium & high Q^2
Q^2 / GeV^2

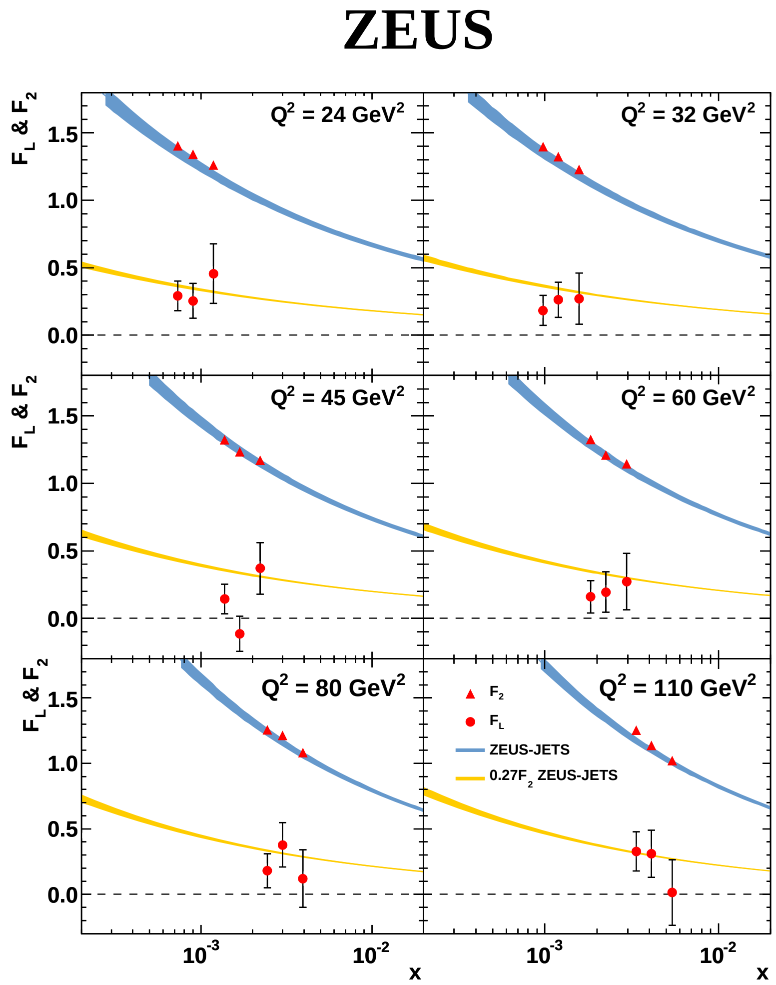
ZEUS
F_L & F_2
Q^2 = 24 GeV^2
Q^2 = 32 GeV^2
Q^2 = 45 GeV^2
Q^2 = 60 GeV^2
Q^2 = 80 GeV^2
Q^2 = 110 GeV^2
F_2
F_L
ZEUS-JETS
0.27F_2 ZEUS-JETS
x

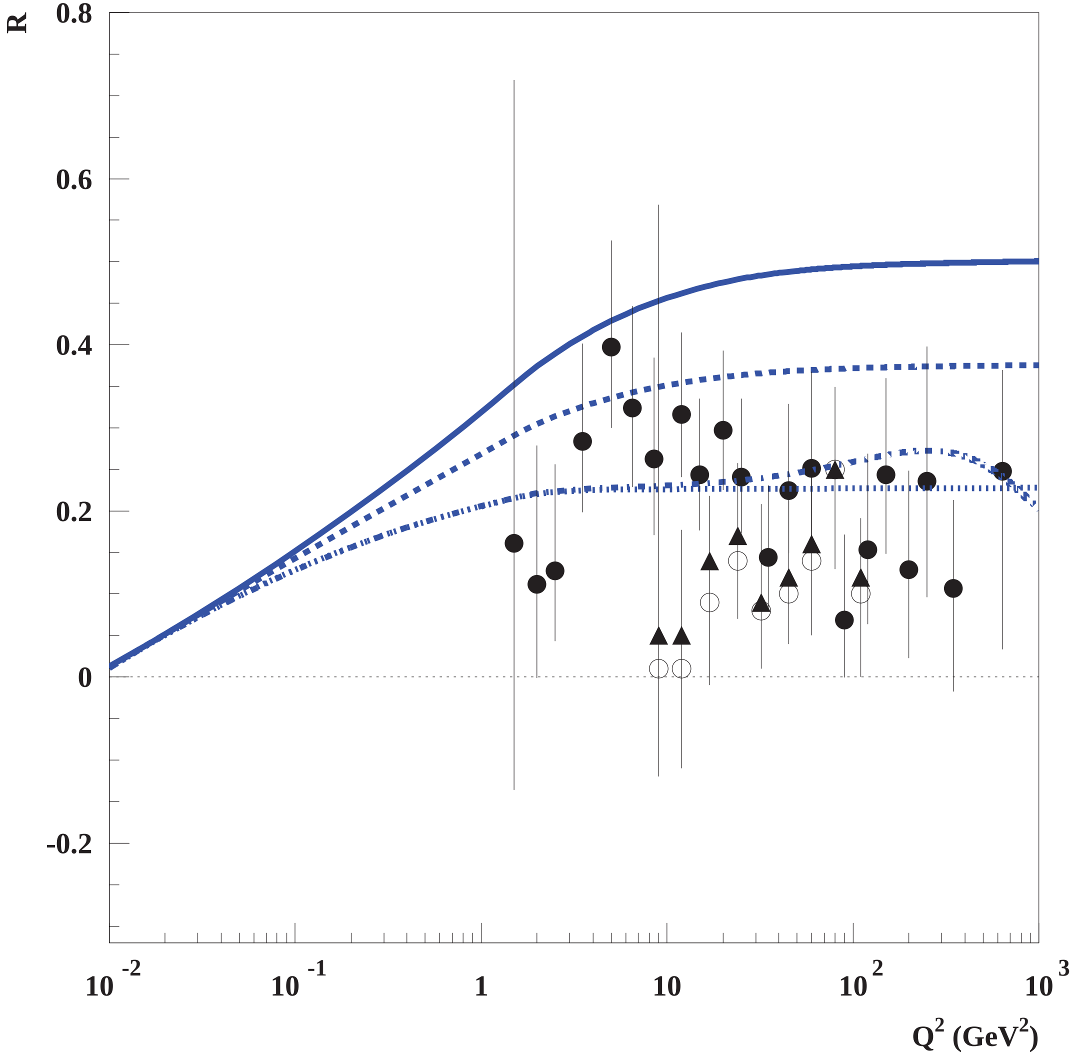

Experiment: $R(Q^2)|_{W \simeq 200 \text{ GeV}}$

H1 (2013)

ZEUS (2014)

Theory (CDP)

$\longleftarrow \quad \rho = 1$

$\longleftarrow \quad \rho = \frac{4}{3}$ (uncertainty principle)

$\longleftarrow \quad \rho = 2$

So far: Model-independently:

$$\sigma_{\gamma^* p} \sim \begin{cases} ln\frac{1}{\eta(W^2,Q^2)} & , \quad \eta(W^2,Q^2) \ll 1 \\ \frac{1}{\eta(W^2,Q^2)} & , \quad \eta(W^2,Q^2) \gg 1 \end{cases}$$

$$R = \begin{cases} 0 & \text{for } Q^2 = 0, \left(\eta = \frac{m_0^2}{\Lambda^2_{\text{sat}}(W^2)}\right), \\ \frac{1}{2\rho} & \quad \text{for } \eta(W^2,Q^2) \gg 1. \end{cases}$$

Interpolation between $\eta(W^2,Q^2) < 1$ and $\eta(W^2,Q^2) > 1$ by explicit ansatz for the dipole cross section.

Simple ansatz for $\sigma_{(q\bar{q})p}$ cross section

Cvetic, Schildknecht, Surrow, Tentyukov (2001)

Kuroda, Schildknecht (2011)

and arXiv: 1606.07862.

$$\sigma_{\gamma^* p}(W^2, Q^2) = \frac{\sigma_{\gamma p}(W^2)}{\lim\limits_{\eta \to \mu(W^2)} I_T^{(1)}\left(\frac{\eta}{\rho}, \frac{\mu}{\rho}\right)} \left(I_T^{(1)}\left(\frac{\eta}{\rho}, \frac{\mu}{\rho}\right) G_T(u) + I_L^{(1)}(\eta, \mu) G_L(u) \right)$$

$$G_{L,T}(u) = \frac{1}{2(1+u)^3} \begin{cases} 2u^3 + 6u^2, & (L), \\ 2u^3 + 3u^2 + 3u, & (T). \end{cases}$$

$$u = \frac{\xi}{\eta(W^2, Q^2)}; \qquad \mu(W^2) = \frac{m_0^2}{\Lambda_{\text{sat}}^2(W^2)}.$$

$$m_{q\bar{q}}^2 \leq m_1^2(W^2) = \xi \Lambda_{\text{sat}}^2(W^2).$$

$$I_L^{(1)}(\eta,\mu) = \frac{\eta-\mu}{\eta}$$

$$\times \left(1 - \frac{\eta}{\sqrt{1+4(\eta-\mu)}} \ln \frac{\eta(1+\sqrt{1+4(\eta-\mu)})}{4\mu - 1 - 3\eta + \sqrt{(1+4(\eta-\mu))((1+\eta)^2-4\mu)}}\right),$$

$$I_T^{(1)}(\eta,\mu) = \frac{1}{2}\ln\frac{\eta-1+\sqrt{(1+\eta)^2-4\mu}}{2\eta} - \frac{\eta-\mu}{\eta} + \frac{1+2(\eta-\mu)}{2\sqrt{1+4(\eta-\mu)}}$$

$$\times \ln \frac{\eta(1+\sqrt{1+4(\eta-\mu)})}{4\mu - 1 - 3\eta + \sqrt{(1+4(\eta-\mu))((1+\eta)^2-4\mu)}}.$$

Comparison with experiment:

Kuroda, Schildknecht (2011)

- $\sigma_{\gamma p}(W^2)$ from Particle Data Group parameterization

- $\Lambda^2_{sat}(W^2) = C_1 \left(\frac{W^2}{W_0^2} + 1\right)^{C_2} \cong$ const $\left(\frac{W^2}{1GeV^2}\right)^{C_2}$

$$C_1 = 1.95 GeV^2$$

$$W_0^2 = 1081 GeV^2$$

$$C_2 = 0.27(0.29)$$

$$m_0^2 = 0.15 GeV^2$$

$$m_1^2(W^2) = \xi \Lambda^2_{sat}(W^2) = 130 \Lambda^2_{sat}(W^2)$$

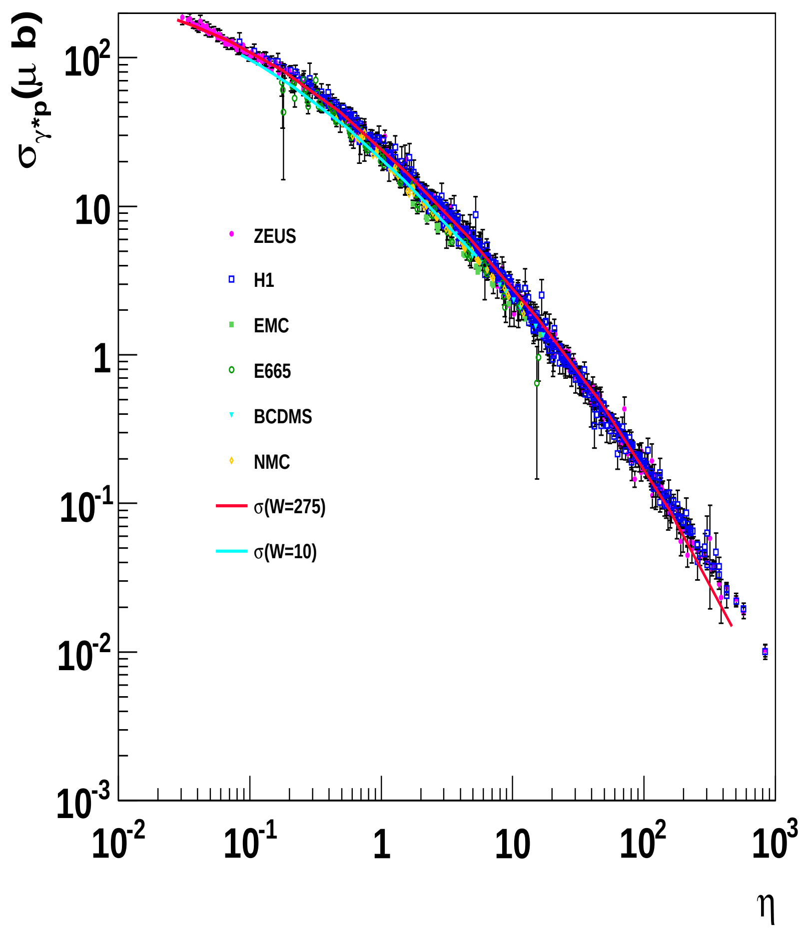

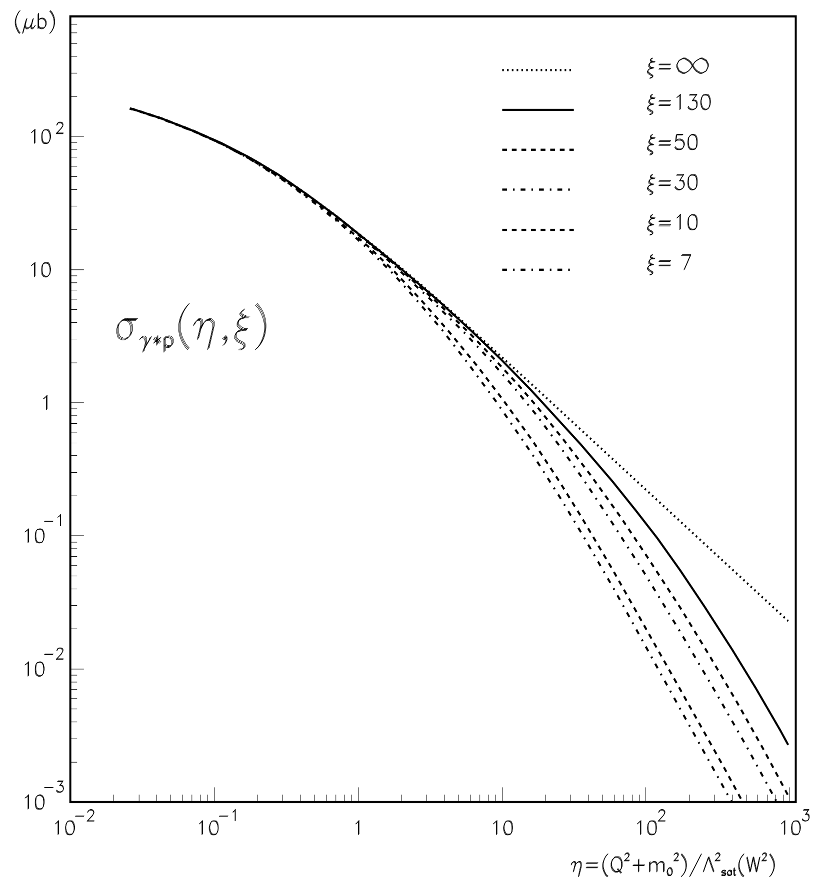

$$m_{q\bar{q}}^2 < m_1^2(W^2) = \xi \Lambda_{sat}^2(W^2)$$

$$\text{For e.g.}\,\eta \simeq 1 \text{ and } \xi = 10 : m_{q\bar{q}} \lesssim \begin{cases} 3GeV & (Q^2 \cong 1GeV^2), \\ 8GeV & (Q^2 \cong 70GeV^2). \end{cases}$$

Reduced Cross Section

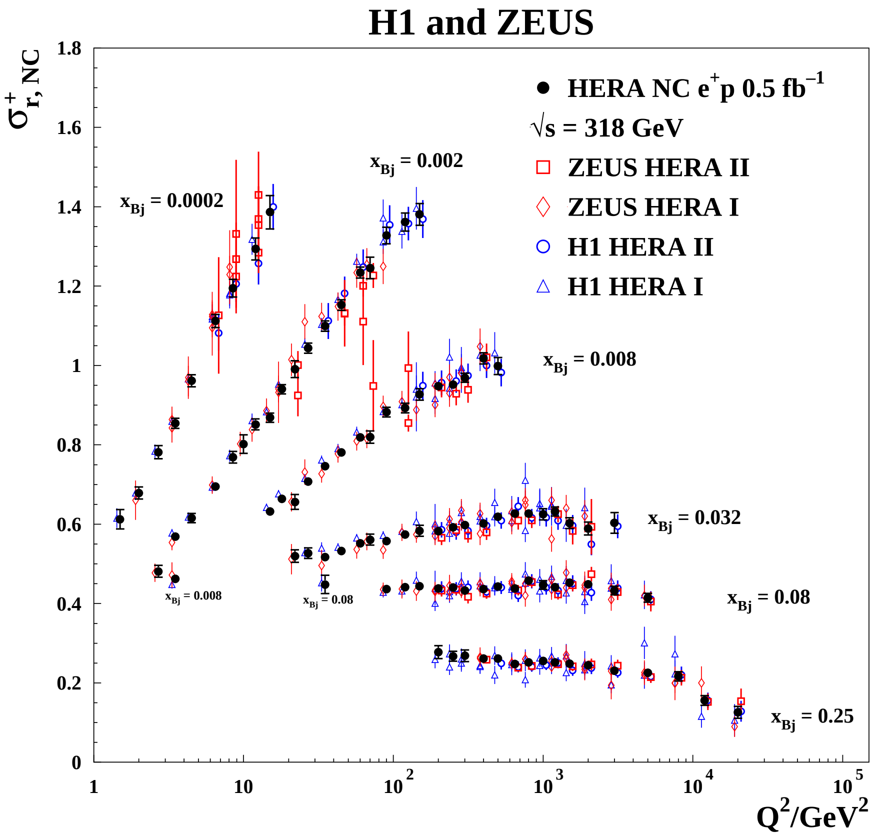

H1 and ZEUS Collaborations

arXiv:1506.06042

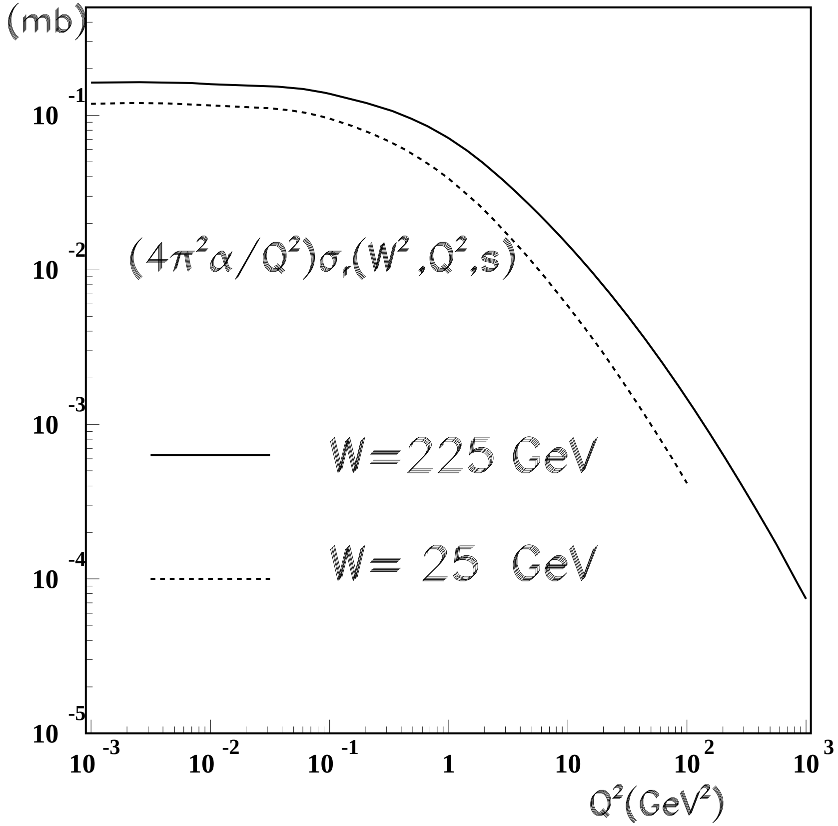

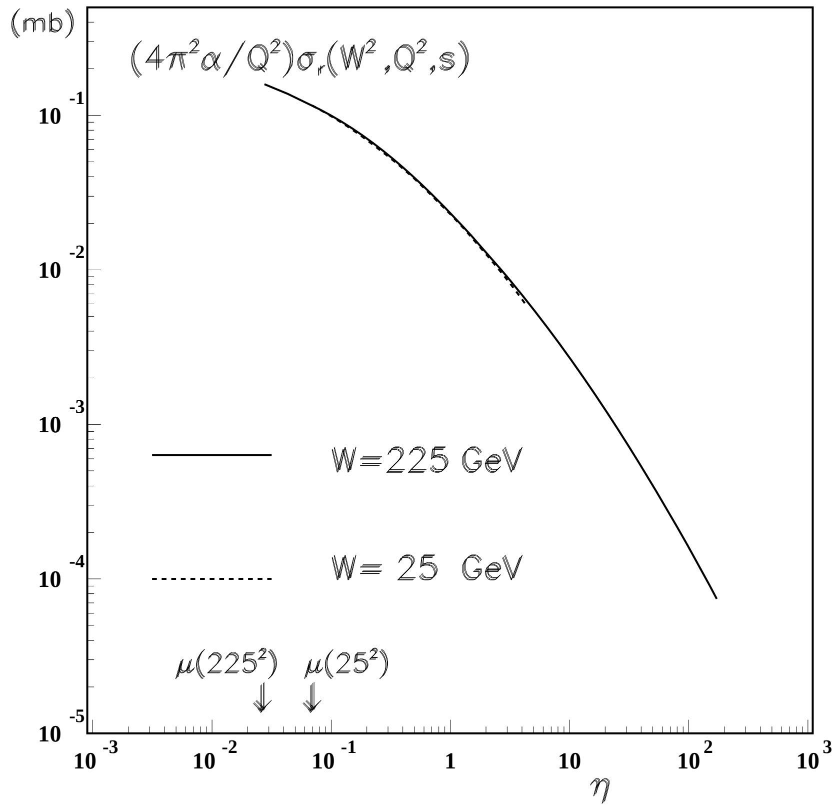

Scaling in $\eta(W^2, Q^2)$ of the reduced cross section:

$$\frac{4\pi^2\alpha}{Q^2}\sigma_r(W^2, Q^2, s) = \sigma_{\gamma_T^* p}(W^2, Q^2)\left(1 + \frac{y^2}{1+(1-y)^2} \; \frac{R(W^2, Q^2)}{1+R(W^2, Q^2)}\right)$$
$$\cong \sigma_{\gamma^* p}(W^2, Q^2)$$

Kuroda, Schildknecht, arXiv:1606.07862

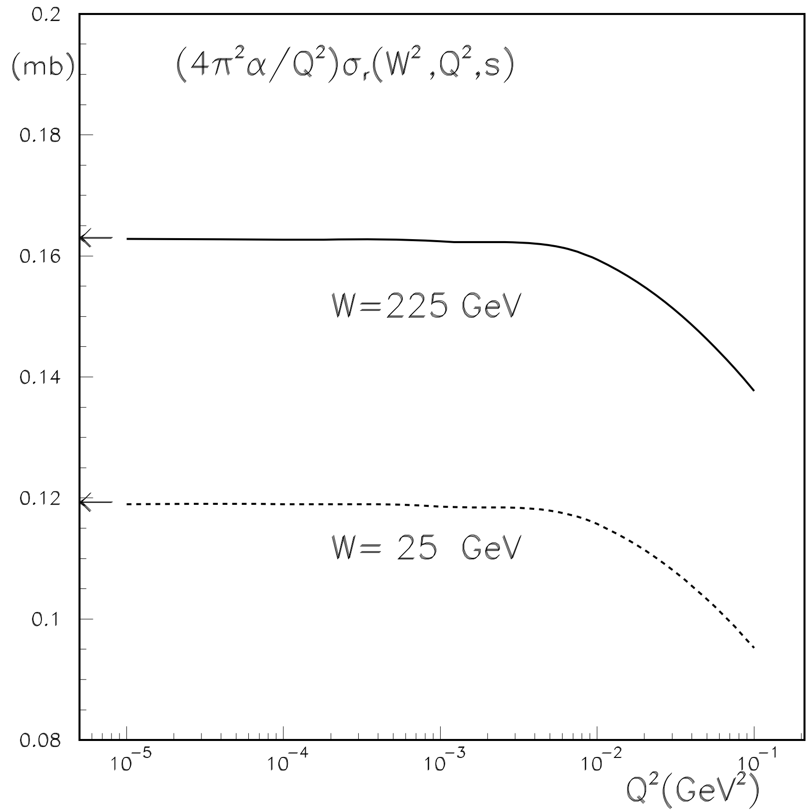

0.2
(mb)
$(4\pi^2\alpha/Q^2)\sigma_r(W^2,Q^2,s)$
0.18
0.16
W=225 GeV
0.14
0.12
W= 25 GeV
0.1
0.08
10^{-5}
10^{-4}
10^{-3}
10^{-2}
10^{-1}
$Q^2(GeV^2)$

Comparison with the experimental data for F_2 (Kuroda, Schildknecht, 2010)

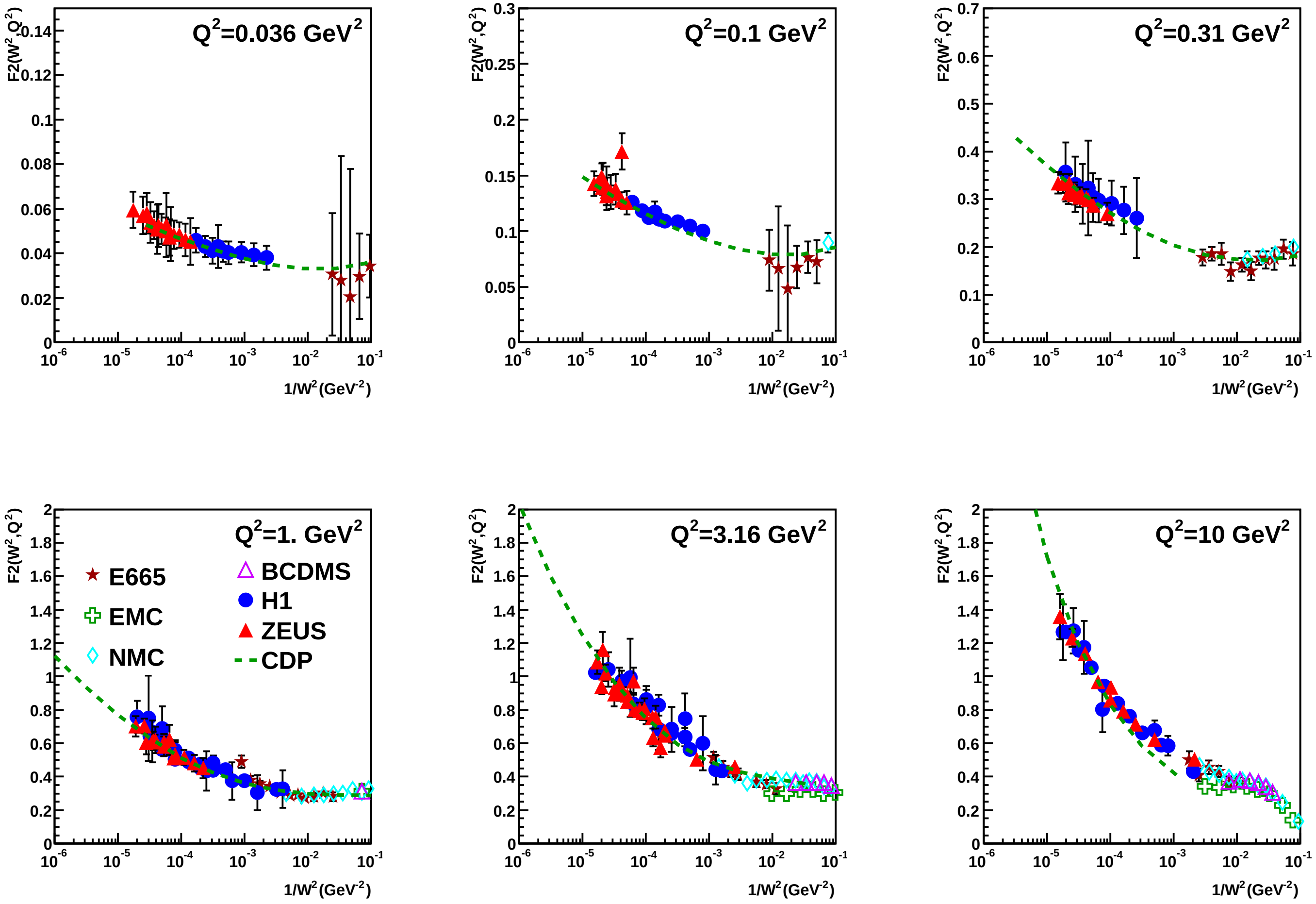

Saturation limit: $\lim\limits_{\substack{W^2\to\infty \\ Q^2\text{fixed}}} \frac{F_2(x\cong Q^2/W^2, Q^2)}{\sigma_{\gamma p}(W^2)} = \frac{Q^2}{4\pi^2\alpha}$

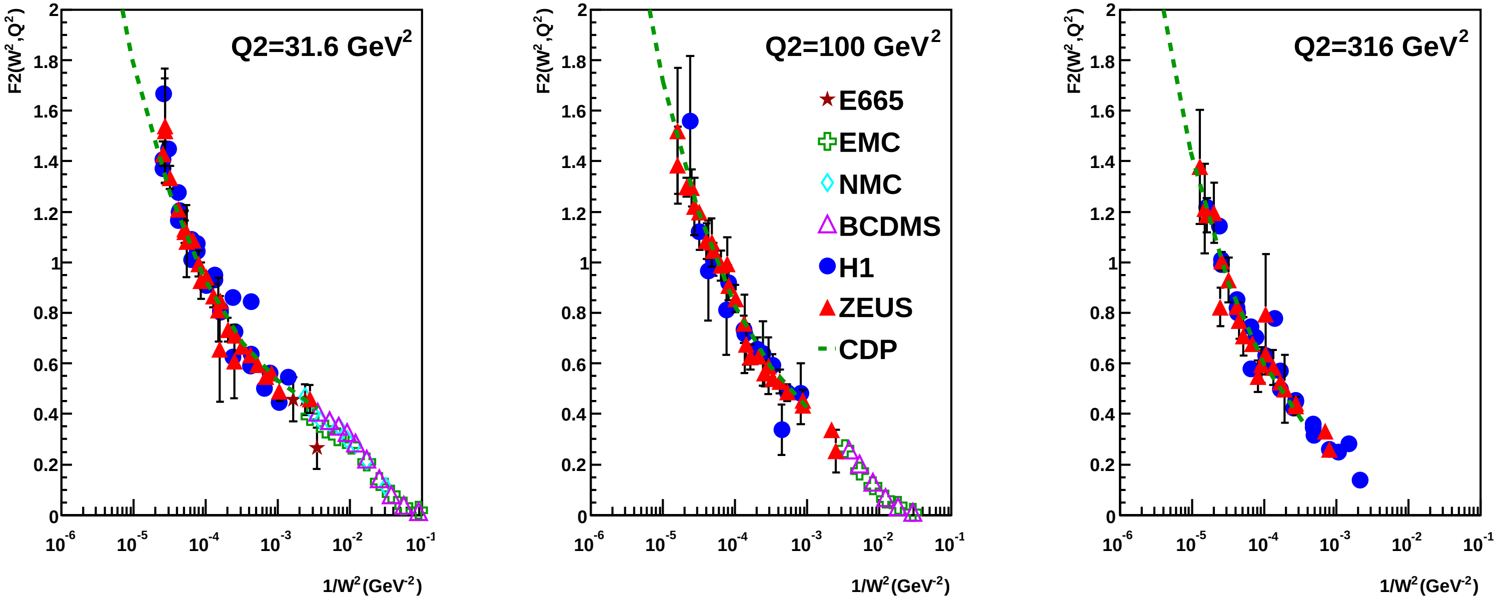

Q2=31.6 GeV^2
Q2=100 GeV^2
Q2=316 GeV^2
F2(W^2,Q^2)
1/W^2(GeV^{-2})
E665
EMC
NMC
BCDMS
H1
ZEUS
CDP

A Remark on : $F_2(W^2)$ in terms of gluon distribution:

$$F_2(W^2 = \frac{Q^2}{x}) = \frac{(2\rho+1)\sum Q_q^2}{3\pi}\xi_L^{C_2}\alpha_s(Q^2)G(x,Q^2) \qquad \eta(W^2,Q^2) \gg 1.$$

$$= \frac{(2\rho+1)\sum Q_q^2}{3\pi}\frac{1}{8\pi^2}\sigma_L^{(\infty)}\Lambda_{sat}^2(W^2). \qquad \text{color transparency}$$

(upon using $F_2 = f_2\left(\frac{W^2}{1GeV^2}\right)^{0.29} = \frac{(2\rho+1)\sum Q_q^2}{3\pi}\frac{1}{8\pi^2}\sigma_L^{(\infty)}\Lambda_{sat}^2(W^2)$.)

Saturation behavior:

$$F_2(W^2,Q^2) \sim Q^2\sigma_L^{(\infty)}\ln\frac{\Lambda_{\rm sat}^2(W^2)}{Q^2+m_0^2}$$

$$\sim Q^2\sigma_L^{(\infty)}\ln\left(\frac{\alpha_s(Q^2)G(x,Q^2)}{\sigma_L^{(\infty)}(Q^2+m_0^2)}\right), \qquad \eta(W^2,Q^2) \ll 1.$$

saturation

Logarithmic dependence on gluon distribution in saturation limit.

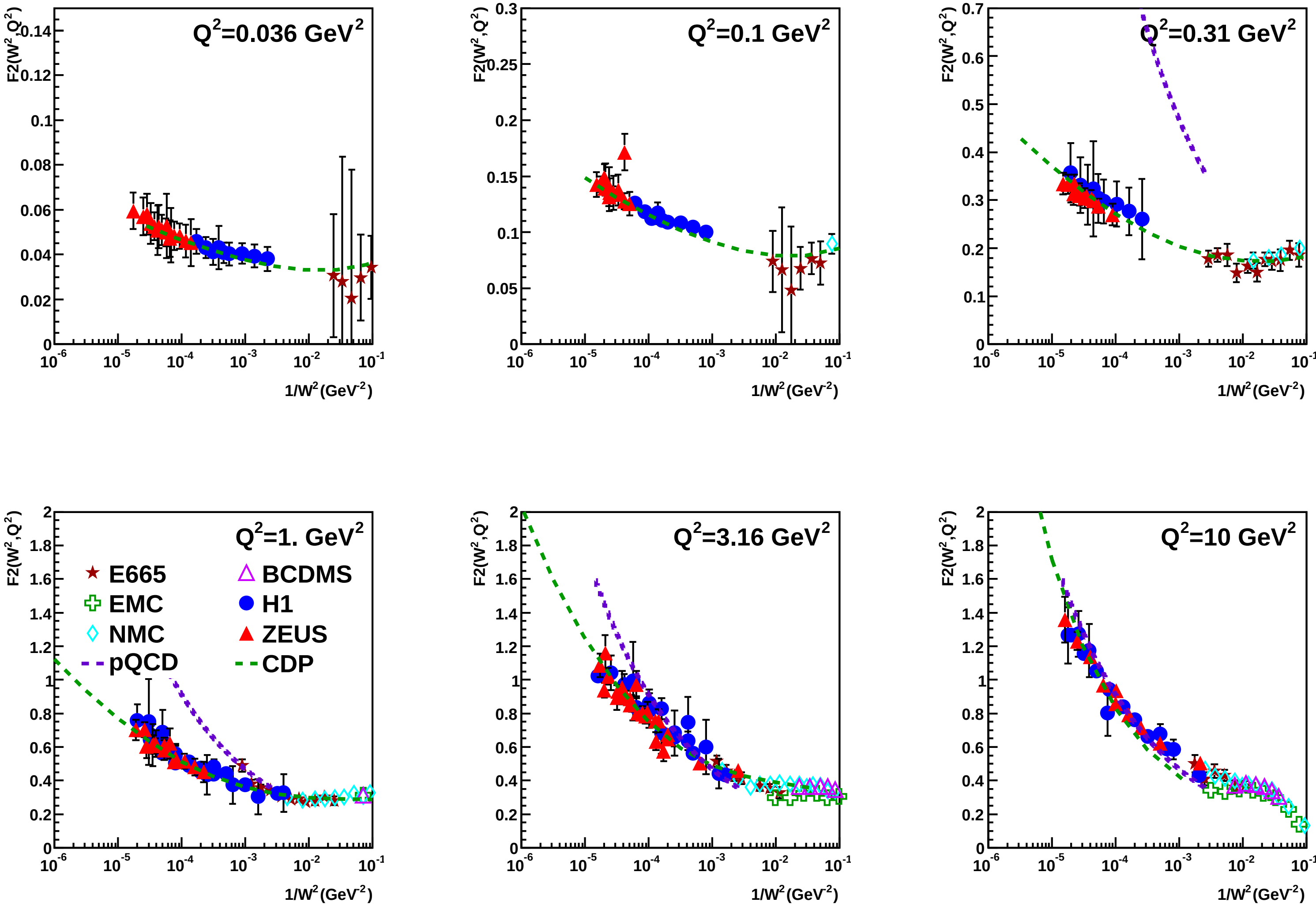

CDP and pQCD-improved parton model

2. Photo- and Electroproduction of J/ψ and Y

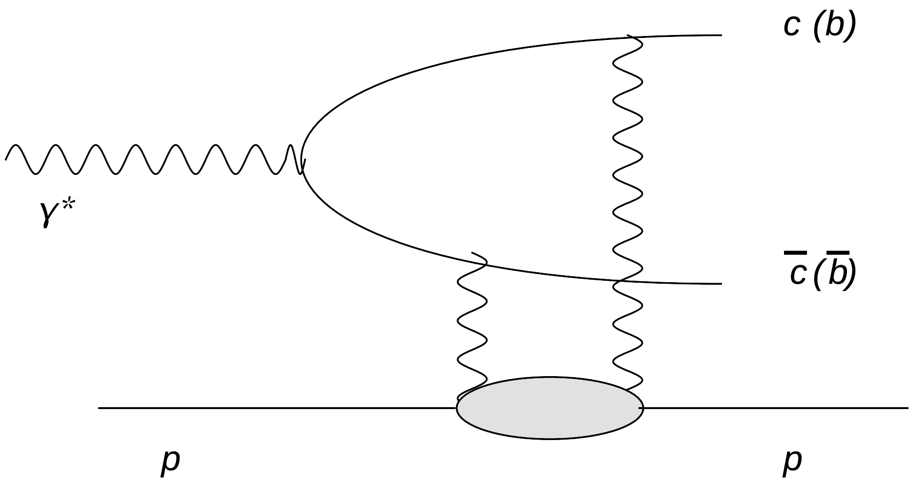

$$\frac{d\sigma_{\gamma^* p \to J/\psi p}}{dt}(W^2, Q^2)\bigg|_{t=0} = \int_{\Delta M^2_{J/\psi}} dM^2 \int_{Z_-}^{Z_+} dz \frac{d\sigma_{\gamma^* p \to (c\bar{c})^{J=1} p}}{dt dM^2 dz}(W^2, Q^2, z, m_c^2, M^2)$$

$$z_\pm = \frac{1}{2} \pm \sqrt{1 - 4\frac{m_c^2}{M^2}}, \qquad \Delta M^2_{J/\psi} \cong 3GeV^2$$

Threshold: $z = \frac{1}{2}$; $\quad M^2 = 4m_c^2 = M^2_{J/\psi}$

$$\frac{d\sigma_{\gamma^* p \to J/\psi p}}{dt}(W^2, Q^2)\Big|_{t=t_{min}\simeq 0} = \frac{3}{2}\frac{1}{16\pi}\frac{\alpha R^{(J/\psi)}}{3\pi}$$

$$\times \frac{\Lambda^4_{sat}(W^2)\Delta F^2(m_c^2, \Delta M^2_{J/\psi})(\sigma^{(\infty)}(W))^2}{(Q^2+M^2_{J/\psi})^3\left(1+\frac{\Lambda^2_{sat}(W^2)}{Q^2+M^2_{J/\psi}}\right)^2} \qquad (R^{J/\psi}=\tfrac{4}{3})$$

$$\sim \begin{cases} \frac{\Lambda^4_{sat}(W^2)(\sigma^{(\infty)}(W))^2}{(Q^2+M^2_{J/\psi})^3} & \text{for } Q^2+M^2_{J/\psi} \gg \Lambda^2_{sat}(W^2) \\ \frac{\left(\sigma^{(\infty)}(W)\right)^2}{(Q^2+M^2_{J/\psi})} \sim \frac{(\ln W^2)^2}{(Q^2+M^2_{J/\psi})} & \text{for } \Lambda^2_{sat}(W^2) \gg Q^2+M^2_{J/\psi} \end{cases}$$

saturation limit.

Note: $\Lambda^2_{\mathrm{sat}}(\mathrm{W}^2) \simeq 10\mathrm{M}^2_{\mathrm{J}/\psi}$ for $\mathrm{W} \simeq 30.000\mathrm{GeV}$.

$$\sim \frac{\Lambda^4(\mathrm{W}^2)(\sigma^{(\infty)}(\mathrm{W}))^2}{\mathrm{M}^6_{\mathrm{J}/\psi}\left(1+\frac{\Lambda^2_{\mathrm{sat}}(\mathrm{W}^2)}{\mathrm{M}^2_{\mathrm{J}/\psi}}\right)^2}, \quad \text{for} \quad Q^2 \ll M^2_{J/\psi}.$$

$\boldsymbol{\sigma(\gamma^* p \rightarrow J/\psi p)}$ **as a function of** $\boldsymbol{Q^2}$**,** $\quad \boldsymbol{W = 90 GeV}$**.**

Kuroda, Schildknecht (2006)

Phys. Lett. B. 638 (2006) 473

$$\sigma(\gamma^* p \rightarrow J/\psi p) \sim \frac{1}{(Q^2+M^2_{J/\psi})^3} \qquad \left(Q^2 + M^2_{J/\psi} \gg \Lambda^2_{sat}(W^2)\right)$$

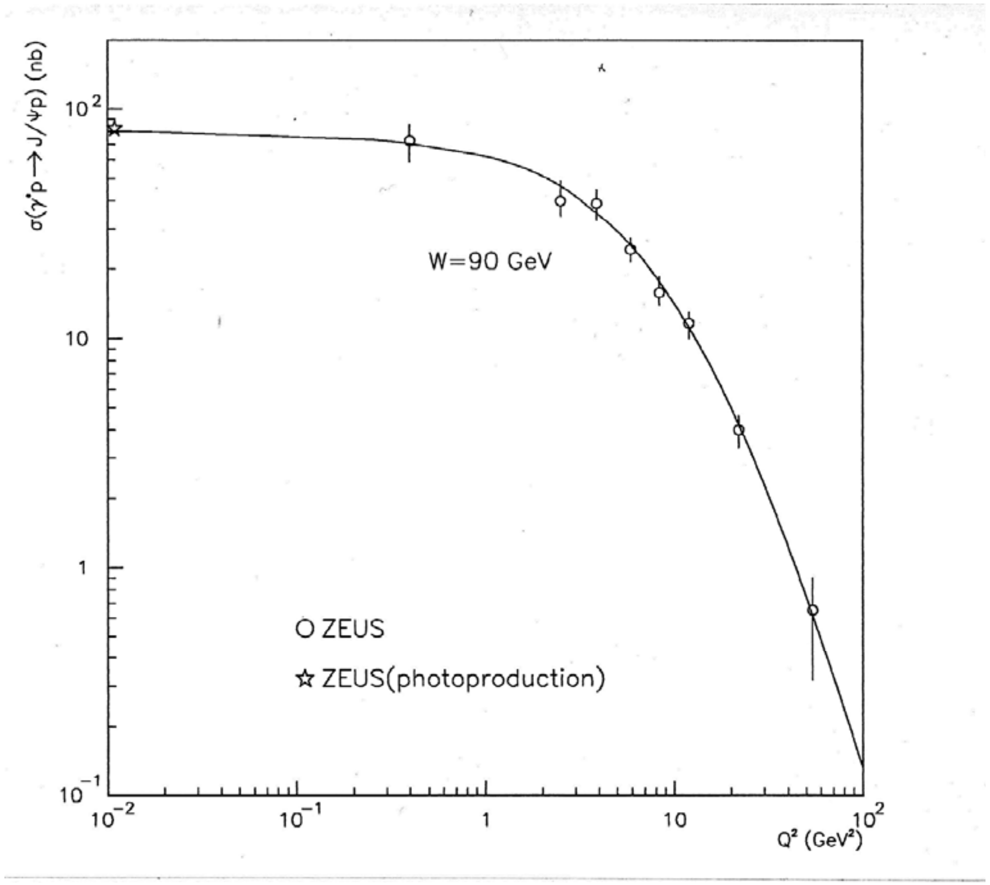

Photoproduction: $\boldsymbol{\sigma(\gamma p \to J/\psi p) \sim \frac{\Lambda^4_{sat}(W^2)}{\left(1+\frac{\Lambda^2_{sat}(W^2)}{M^2_{J/\psi}}\right)^2}(\ln W^2)^2}$

Illustration $\boldsymbol{\sigma(\gamma p \to J/\psi p) \sim \Lambda^4_{sat}(W^2)}$

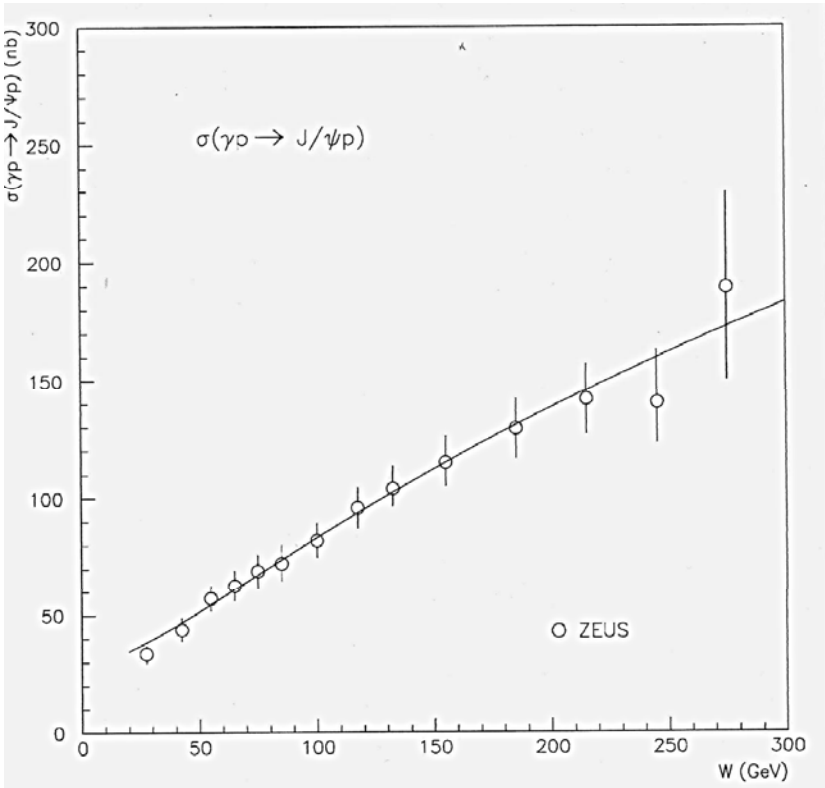

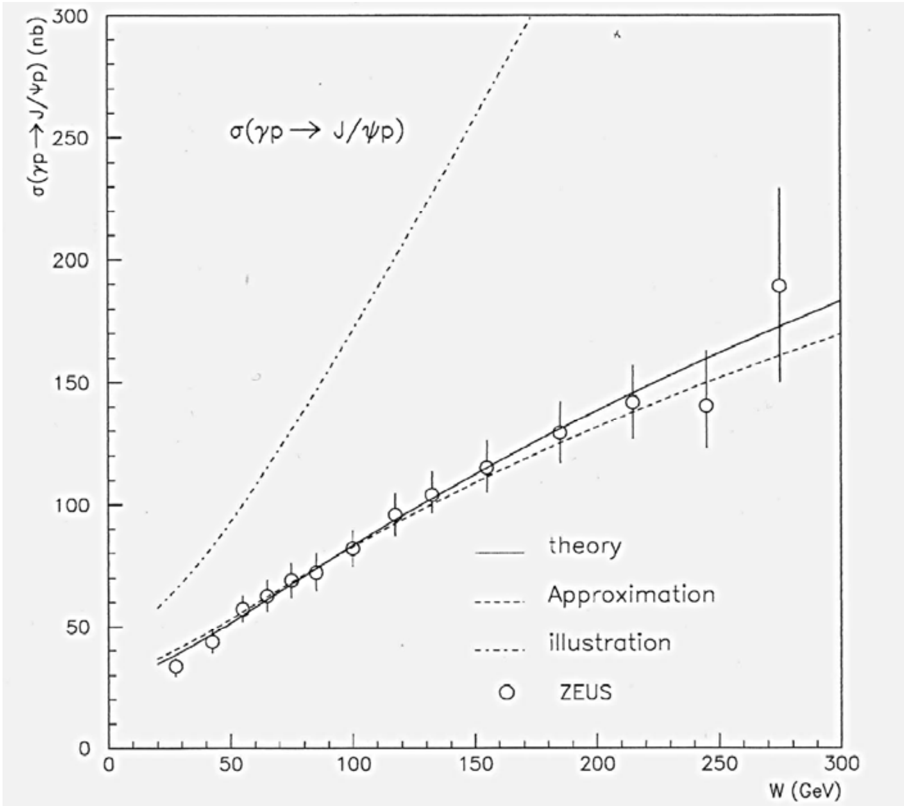

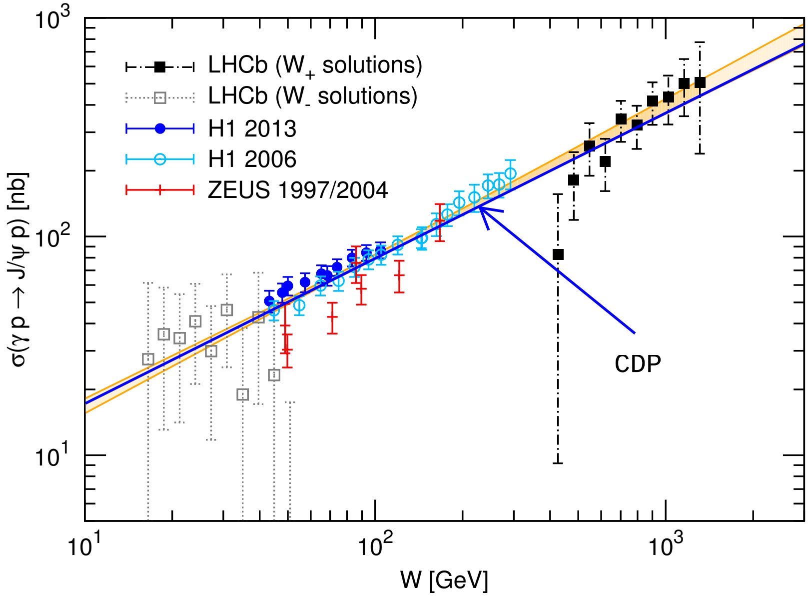

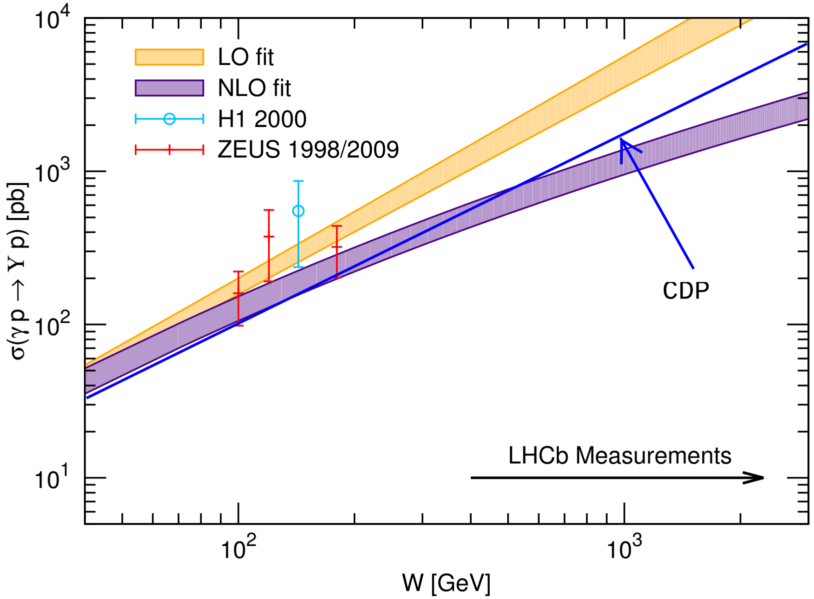

CDP: Kuroda, Schildknecht (2006)

Phys. Lett. B 638 (2006) 473

Jones et al., arXiv:1307.7099

3. The Neutrino-Nucleon Cross Section at ultrahigh energy in the Color Dipole Picture

$$\sigma_{\nu N}(E) = \frac{G_F^2}{2\pi}\int_{Q^2_{min.}}^{s-M_p^2} dQ^2 \left(\frac{M_W^2}{Q^2+M_W^2}\right)^2 \int_{M_p^2}^{s-Q^2} \frac{dW^2}{W^2}\sigma_r(x,Q^2).$$

e.g. Goncalves and Hepp (2011)

$$s = 2M_pE + M_p^2 \cong 2M_pE,$$
$$x = \frac{Q^2}{2qP} = \frac{Q^2}{W^2+Q^2-M_p^2} \cong \frac{Q^2}{W^2},$$

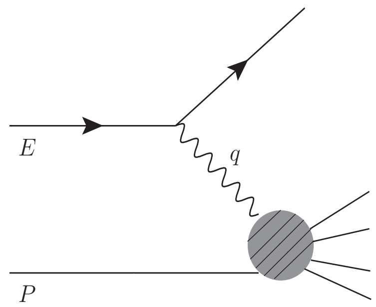

$$\sigma_r(x,Q^2) = \frac{1+(1-y)^2}{2}F_2^{\nu}(x,Q^2) - \frac{y^2}{2}F_L^{\nu}(x,Q^2) + y(1-\frac{y}{2})xF_3^{\nu}(x,Q^2).$$

$$y = \frac{Q^2}{2M_pEx} \cong \frac{W^2}{s}.$$

For $s \gg M_W^2 \approx 10^4\mathrm{GeV}^2$,

dominant contribution from $Q^2 \cong M_W^2$,

$$x \cong \frac{M_W^2}{s} \ll 0.1,$$

Connection to ep deep inelastic scattering (DIS)

HERA (1990 to 2007): DIS at low values of

$$x \equiv x_{bj} \simeq \frac{Q^2}{W^2}, \text{ where}$$
$$5 \cdot 10^{-4} \leq x \leq 10^{-1}$$
$$0 \leq Q^2 \leq 100\text{GeV}^2$$

For n_f actively contributing quark flavors:

$$\frac{1}{n_f} F_{2,L}^{\nu N}(x, Q^2) = \frac{1}{\sum_q Q_q^2} F_{2,L}^{eN}(x, Q^2);$$

$$F_{2,L}^{\nu N}(x, Q^2) = \frac{n_f}{\sum_q^{n_f} Q_q^2} F_{2,L}^{eN}(x, Q^2), \quad \text{with } \frac{n_f}{\sum_q^{n_f} Q_q^2} = \frac{5}{18} \quad (\text{for } n_f = 4).$$

$$F_2^{ep}(x, Q^2) = \frac{Q^2}{4\pi^2 \alpha} \sigma_{\gamma^* p}(W^2, Q^2).$$

The Neutrino-Nucleon Cross Section in the CDP

$$\sigma_{\nu N}(E) = \frac{G_F^2 M_W^4}{8\pi^3\alpha}\frac{n_f}{\sum_q Q_q^2}\int_{Q^2_{Min}}^{s-M_p^2} dQ^2 \frac{Q^2}{(Q^2+M_W^2)^2} \times \int_{M_p^2}^{s-Q^2}\frac{dW^2}{W^2}\frac{1}{2}(1+(1-y)^2)\sigma_{\gamma^* p}(\eta(W^2,Q^2)).$$

Kuroda, Schildknecht, arXiv:1305.0440v3, Phys. Rev. D88 (2013) 053007

$$r(E) = \frac{\sigma_{\nu N}(E)_{\eta(W^2,Q^2)<1}}{\sigma_{\nu N}(E)}.$$

Contribution from saturation region

$$r(E) < \bar{r}(E),$$

$$\bar{r}(E) = \frac{2\int_{Q^2_{Min}}^{Q^2_{Max}(s)} dQ^2 \frac{Q^2}{(Q^2+M_W^2)^2}\int_{W^2(Q^2)_{Min}}^{s-Q^2}\frac{dW^2}{W^2}\ln\frac{1}{\eta(W^2,Q^2)}}{\int_{Q^2_{Min}}^{s-M_p^2} dQ^2 \frac{Q^2}{(Q^2+M_W^2)^2}\int_{M_p^2}^{s-Q^2}\frac{dW^2}{W^2}\frac{1}{2\eta(W^2,Q^2)}}.$$

$$r(E) < \bar{r}(E) = \frac{1}{2}\frac{\Lambda^2_{sat}(s)}{M_W^2} = \begin{cases} 1.74\times 10^{-3} & \text{for } E = 10^6\,\text{GeV} \\ 2.51\times 10^{-2} & \text{for } E = 10^{10}\,\text{GeV} \\ 3.63\times 10^{-1} & \text{for } E = 10^{14}\,\text{GeV} \end{cases}.$$

Note: Ice Cube Experiment, $E \lesssim 10^6 GeV$

The (charged-current) neutrino-nucleon cross section, $\sigma_{\nu N}(E)$, (based on $\sigma_{\gamma^* p}(\eta(W^2, Q^2))$ from CDP) as a function of the neutrino energy $E_\nu(GeV)$.

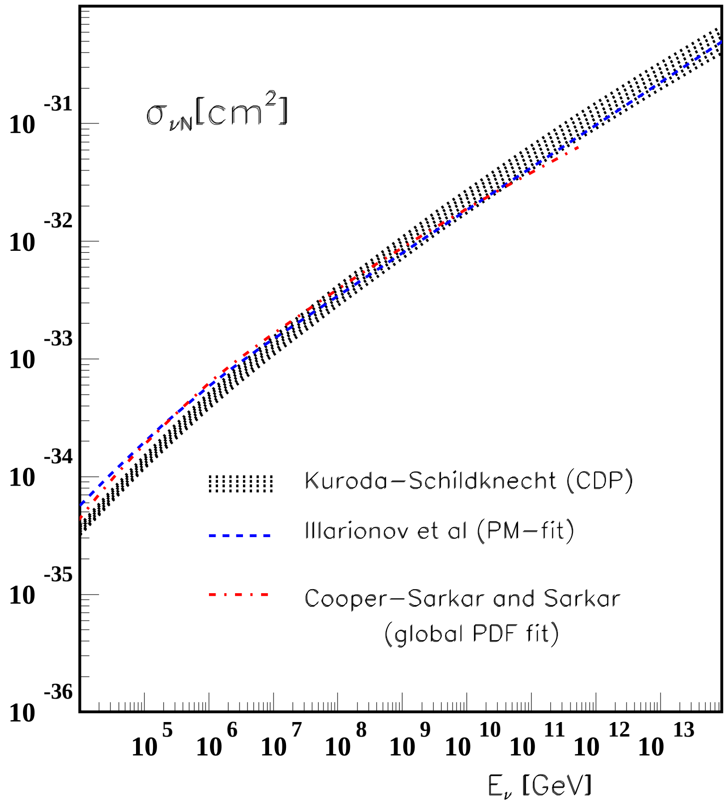

Comparison with "Froissart-inspired" ansatz

Heisenberg (1953):

Lorentz-contracted sphere with exponentially decreasing edge

Minimum "blackness" necessary for particle production.

Collision radius then given by radius of "suffiently black" region.

$\sigma_{hN}(W^2) \sim (\ln W^2)^2$

Froissart (1961):

From unitarity and analyticity, upper bound,

$\sigma_{hN}(W^2) < (\ln W^2)^2$.

"Froissart-inspired ansatz":

$$F_2^{ep}(x_1, Q^2) \sim \sum_{n,m=0,1,2} a_{nm}(\ln Q^2)^n(\ln(1/x))^m$$

Block et al. (2006 to 2013)

Fit to HERA low-x data with seven fit parameters.

Comparison of $\boldsymbol{\sigma_{\nu N}(E)}$ from the CDP with the results from the "Froissart-inspired" ansatz

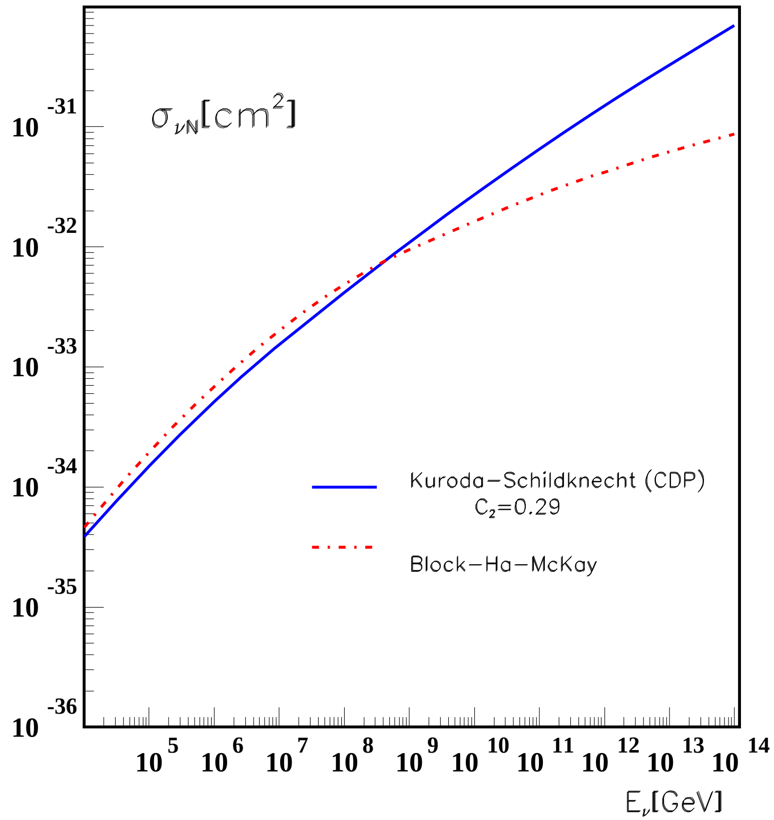

On suppression see also
e.g. Machado (2011)

The neutrino-nucleon cross section in the CDP for (unrealistic!) ultra-ultra-high energies, $E \leq 10^{24}$GeV. Reduced growth of cross section for $E \gg 10^{12}$ GeV

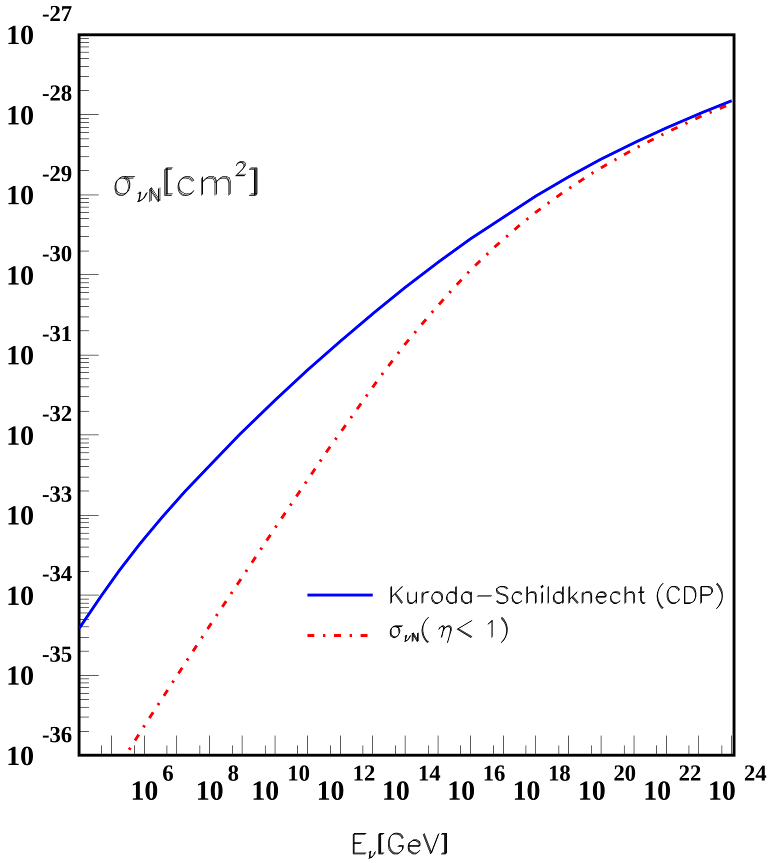

$$\sigma^{(c)}_{\nu N}(E) = \sigma^{(c)}_{\nu N}(E)_{\eta(W^2,Q^2)<1} + \sigma_{\nu N}(E)^{(c)}_{\eta(W^2,Q^2)>1}$$

4. Conclusions

Deep Inelastic Scattering (DIS)

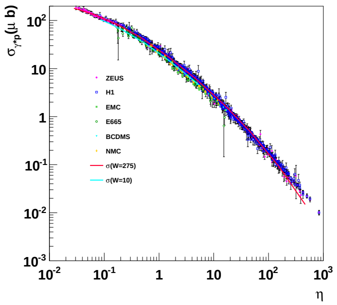

- The empirically observed low-x ($x_{bj} \cong \frac{Q^2}{W^2} \leq 0.1$) scaling behavior,

  $$\sigma_{\gamma^* p}(W^2, Q^2) = \sigma_{\gamma^* p}\left(\eta(W^2, Q^2)\right),$$

  where $\eta(W^2, Q^2) = \frac{Q^2 + m_0^2}{\Lambda^2_{\rm sat}(W^2)}$,

  $$\Lambda^2_{\rm sat}(W^2) = C_1 \left(\frac{W^2}{1\mathrm{GeV}^2}\right)^{C_2},$$

  is a consequence of the color-gauge-invariant $q\bar{q}$-dipole interaction with the color field in the nucleon.

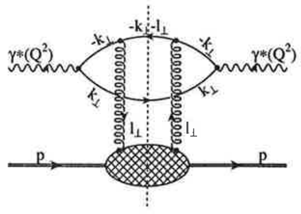

(a)

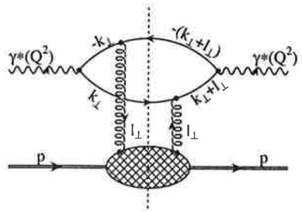

(b)

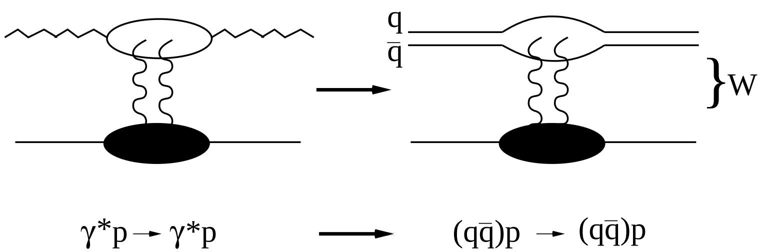

- For $\eta(W^2, Q^2) \gg 1$, color transparency, $\sigma_{(q\bar{q})p} \sim \vec{r}_\perp^{\,2}$, implies $\sigma_{\gamma^* p} \sim \frac{1}{\eta}$.

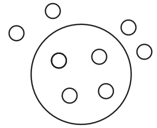

- For $\eta(W^2, Q^2) \ll 1$, saturation, $\sigma_{(q\bar{q})p} \sim \sigma^{(\infty)}(W^2)$, implies $\sigma_{\gamma^* p} \sim \sigma^{(\infty)}(W^2) \ln \frac{1}{\eta}$, i. e. hadronlike $\ln^2 W^2$ dependence at any Q^2 fixed.

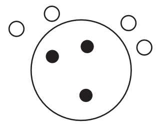

- $R(W^2, Q^2) = \frac{\sigma_{\gamma^*_L p}(\eta(W^2,Q^2))}{\sigma_{\gamma^*_T p}(\eta(W^2,Q^2))} = \frac{1}{2\rho}$ for $\eta \gg 1$.

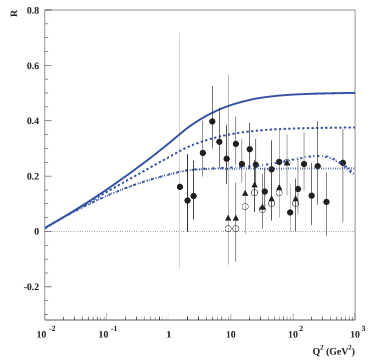

- Detailed model essentially based on a parameterization of

$$\Lambda^2_{\text{sat}}(W^2) = C_1 \left(\frac{W^2}{1\text{GeV}^2} \right)^{C_2}$$

shows agreement with all DIS data at low x, including $Q^2 = 0$ photoproduction.

J/ψ and Y

- Applying quark-hadron duality to $c\bar{c}$ and $b\bar{b}$ photo- and electroproduction yields parameter-free predictions for J/ψ and Y production.
- The presently observed strong rise with energy saturates into a $(logW^2)^2$ dependence at asymptotic (ultrahigh) energies.

Neutrino-Nucleon Cross Section

- Predictions for the charged-current neutrino-nucleon cross section based on the CDP are consistent with results obtained from pQCD fits ($E \le 10^{12}$ GeV).
- The results based on the CDP disagree with results from the "Froissart-inspired" ansatz that predicts a strong suppression of the neutrino-nucleon cross section for energies $E \ge 10^9$ GeV
- A suppression of the cross section, i.e., a weaker growth with increasing energy, only occurs at unrealistically high ("ultra-ultra-high") energies of $E \gtrsim 10^{12}$ GeV